Damage evaluation and corrosion detection in concrete by acoustic emission

M. Ohtsu & Y. Tomoda
Kumamoto University, Kumamoto, Japan

T. Suzuki
Nihon University, Kanagawa, Japan

ABSTRACT: Acoustic emission (AE) techniques have been extensively studied and applied to nondestructive testings (NDT) of concrete and concrete structures. For damage evaluation, AE behavior of concrete under compression could be analyzed, applying the rate process theory. Based on Loland's model in damage mechanics, a relation between AE rate and the damage parameter is correlated. By quantifying intact moduli of elasticity of concrete from the database on the relationship, relative damages of concrete in existing structures are successfully estimated by the compression test of concrete samples. The technique is applied to estimate concrete samples of recycled aggregate. The deteriorated degree of recycled concrete is reasonably estimated. For corrosion detection, continuous monitoring of AE signals is useful for earlier warning of corrosion in reinforcement. It is demonstrated that the onset of corrosion in reinforcement and the nucleation of corrosion cracking in concrete could be clearly identified by AE parameter analysis.

1 INTRODUCTION

Concrete and concrete structures could deteriorate due to the environmental effects. Consequently, evaluation of deteriorated degree or damage in concrete has been in so great demand that it is necessary to develop quantitative techniques for damage evaluation in concrete.

In the case of diagnostic inspection of concrete structures, mechanic properties of concrete are normally evaluated by taking core samples. However, properties obtained from the compression test have not been directly applied to damage evaluation. In this concern, acoustic emission (AE) is known to be promising to evaluate the degree of damage. The authors have proposed to evaluate AE activity under compressions by introducing the rate-process analysis (Ohtsu, 1992). By calculating an intact modulus of elasticity from the database based on a relation between AE rate and the damage parameter, a procedure to estimate the relative damage of concrete is implemented as Damage evaluation of Concrete by AE raTe-process analysis (DeCAT) (Suzuki and Ohtsu, 2004). In this study, the DeCAT system is applied to estimate a deteriorated degree of concrete samples made of recycled aggregate.

Corrosion of reinforcing steel bars (rebars) is one of critical deteriorations in reinforced concrete. When chloride concentration at rebar exceeds a range of values with a probability for corrosion initiation, a passive film on the surface of rebar is destroyed and corrosion is initiated. Then electrochemical reaction continues with available oxygen and water. Corrosion products on rebar surfaces grow with time and nucleate micro-cracks in concrete. According to the Japanese standard specifications on maintenance (JSCE, 2001), deterioration process is specified as illustrated in Fig. 1.

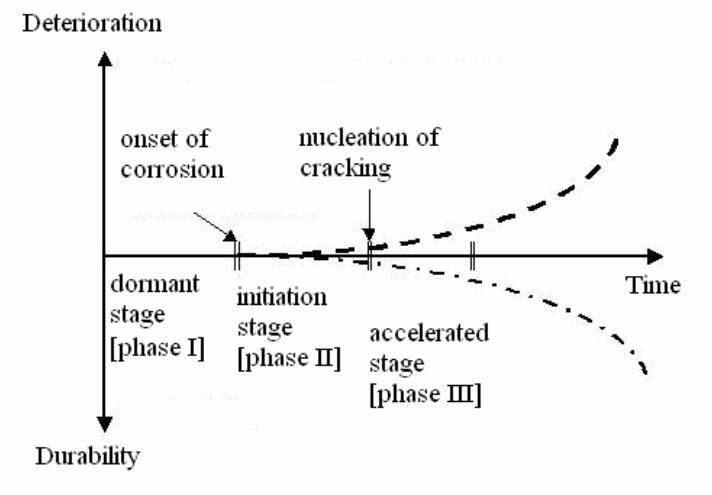

Figure 1. Corrosion process of reinforced concrete.

There exist two transition periods at onset of corrosion and at nucleation of cracks. The former is associated with the transition from the dormant stage (phase I) to the initiation stage (phase II). Corrosion-related damage could begin at this point,

which is normally defined as the initiation time of corrosion. The latter is the transition from the initiation stage (phase II) to the accelerated stage (phase III), and is critically important to assess the durability of reinforced concrete structures. For nondestructive evaluation (NDE) of corrosion, electrochemical techniques of half-cell potential and polarization resistance have been widely employed. Yet, it is known that these techniques can not provide precise information on the two transition periods. As a result, these periods are normally defined by chloride concentration levels at cover thickness in concrete. Here, continuous AE measurement is applied to identify the transition periods at the onset of corrosion and at the nucleation cracking.

2 ANALYSIS OF AE SIGNALS

2.1 *AE rate-process analysis*

AE behavior of a concrete sample under compression is associated with generation of micro-cracks. These micro-cracks are gradually accumulated until final failure. The number of AE events, which correspond to the generation of these cracks, increases acceleratedly along with the accumulation of micro-cracks. It appears that the process is dependent on the number of cracks at a certain stress level as to be subjected to a stochastic process. Therefore, the rate process theory is introduced to quantify AE behavior under compression.

The following equation of the rate process is introduced to formulate the number of AE hits *dN* due to the increment of stress from *V* to *V+dV*,

$$f(V)dV = \frac{dN}{N} \tag{1}$$

where *N* is the total number of AE events and *f(V)* is the probability function of AE at stress level V(%). For *f (V)* in Equation1, the following hyperbolic function is assumed,

$$f(V) = \frac{a}{V} + b \tag{2}$$

where *a* and *b* are empirical constants. Here-inafter, the value '*a*' is called the rate, which reflects AE activity at a designated stress level. At a low stress level the probability varies, depending on whether the rate '*a*' is positive or negative. In the case that the rate '*a*' is positive, the probability of AE activity is high at a low stress level, suggesting that concrete is damaged. In the case of the negative rate, the probability is low at a low stress level, revealing that the structure could be in stable condition. Substituting Equation 2 into Equation 1, a relationship between total number of AE events *N* and stress level *V* is obtained as the following equation,

$$N = CV^a \exp(bV) \tag{3}$$

where C is the integration constant.

A damage parameter Ω in damage mechanics can be defined from a relative ratio of the moduli of elasticity (Loland, 1980),

$$\Omega = 1 - \frac{E}{E^*} \tag{4}$$

where *E* is the modulus of elasticity of concrete and *E** is the ideal modulus of elasticity, which is assumed to be intact or completely undamaged. Assigning Ω_0 is the initial damage at the onset of the compression test, the following equation is derived,

$$E_0 = E^*(1-\Omega_0) \tag{5}$$

In the compression test of a concrete sample, a relation between stress and strain is typically plotted as shown in Figure 2 (a). According to Equation 5, the initial modulus of elasticity E_0 is associated with the initial degree of damage Ω_0. Corresponding to the damage Ω_c at the ultimate strain ε_c, the scant modulus of elasticity, E_c, is defined. In this study, the modulus of elasticity, E_0, was estimated as a tangential modulus, after approximating the stress-strain relation by a parabolic function.

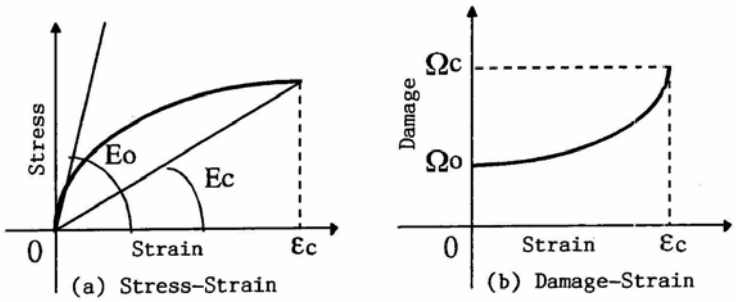

Figure 2. Stress-strain-damage relations under compression.

As given in Equation 5, the initial damage Ω_0 is an index of damage. Still, it is fundamental to know the intact modulus of elasticity of concrete, *E**. But it is not easy to determine the modulus *E** of concrete taken from an existing structure. Consequently, it is attempted to estimate the modulus *E** from AE measurement.

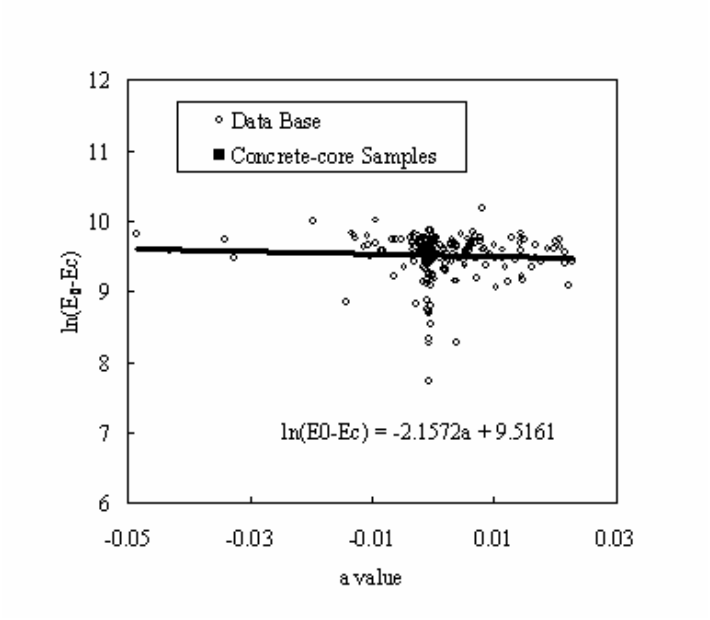

Figure 3. Database on rate 'a' and the modulus.

A correlation between the decrease in the moduli of elasticity, $\log_e(E_0\text{-}E_c)$, and the rate '*a*' derived from AE rate-process analysis is shown in Figure 3. Results of concrete samples previously tested are plotted by open circles and results of core samples recently tested (Suzuki and Ohtsu, 2004) are denoted by solid circles. A linear correlation between $\log_e(E_0\text{-}E_c)$ and the rate '*a*' value is reasonably observed. The decrease in the moduli of elasticity, $E_0\text{-}E_c$, is expressed,

$$E_0 - E_c = E^*(1-\Omega_0) - E^*(1-\Omega_c) = E^*(\Omega_c - \Omega_0) \quad (6)$$

Based on a linear correlation in Figure 3,

$$\log_e(E_0 - E_c) = \log_e[E^*(\Omega_c - \Omega_0)] = xa + c \quad (7)$$

Here, it is assumed that $E_0 = E^*$ when $a = 0$. This allows us to estimate the intact modulus of modulus of concrete, E^*, from AE rate-process analysis as,

$$E^* = E_c + e^c \quad (8)$$

Each time when we conduct the compression test, AE data are added to Figure 3 and the intact modulus is calculated by Equation 8. Thus, Figure 3 works as the database of the DeCAT system.

2.2 *AE parameter analysis*

Characteristics of AE signals were estimated by using two indices of RA value and average frequency. These are defined from such waveform parameters as rise time, maximum amplitude, counts and duration shown in Figure 4, as follows;

RA value = Rise time / Maximum amplitude, (9)

Average frequency = Counts / Duration. (10)

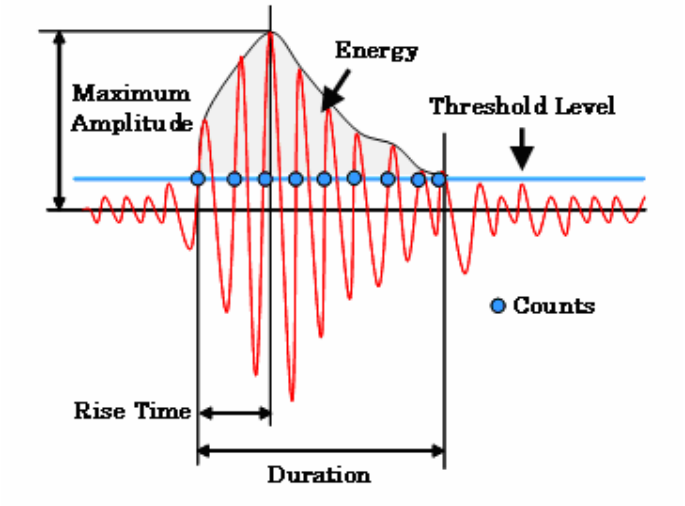

Figure 4. AE wavefrom parameters.

According to the Japan code (JCMS, 2003), AE sources of active cracks are classified into tensile cracks and other-type cracks, based on the relationship between the RA values and the average frequencies, as shown in Figure 5. When the RA value is small and the average frequency is high, AE source is classified as a tensile crack. In the other case, AE source is referred to as a crack other than a tensile crack, including a shear crack. This criterion is applied to classify AE events detected in the corrosion process.

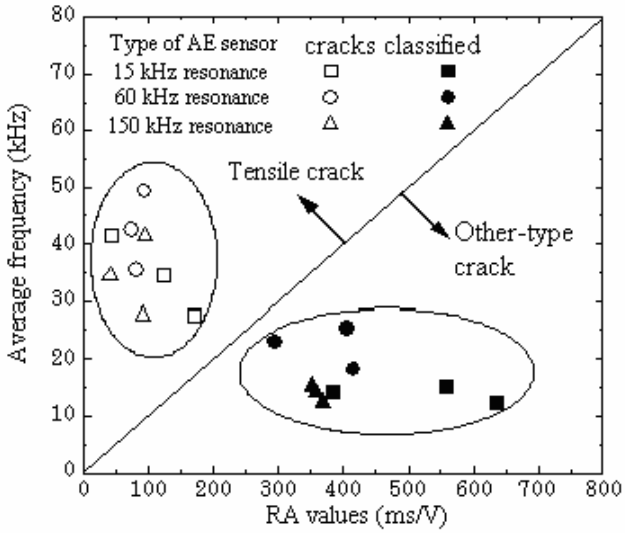

Figure 5. Crack classification by AE indices.

In addition, to evaluate sizes of AE sources, the amplitude distribution of AE events was applied. A relationship between the number of AE events, N, and the amplitudes, A, is statistically represented as,

$$\mathrm{Log}_{10} N = a - b\mathrm{Log}_{10}A, \quad (11)$$

where a and b are empirical constants. The latter is called the b-value, and is often applied to estimate the size distribution of AE sources (Shiotani et al., 2001). In the case that the b-value is large, small AE events are mostly generated. In contrast, the case where the b-values become small implies active nucleation of large AE events.

3 EXPERIMENTS

3.1 *Concrete of recycled aggregate*

Cylindrical samples of 10cm in diameter and 20cm in height were made, which were made of four types of coarse aggregate. These are listed in Table 1. Two types of aggregate were commercially available. One was crushed aggregate and the other was heated and milled. We have recently developed a technique to take coarse aggregate out of concrete, applying the pulse-power, where 100 pulses of 400 kV and 6.4 kJ/shot were discharged in water. Thus, recycled aggregate was taken out of cylindrical concrete samples made of original aggregate, and then was applied to recast concrete samples. In all the types, the maximum gravel size of coarse aggregate was 20 mm, and the water-to-cement ratio was 55%. Air-entrained admixture was added to control the slump vales at around 7 cm and air contents at 6 %. In the table, densities and the absorption coefficients f these aggregates are given. It is realized that densities decrease and the absorptions increases in recycled aggregate, compared with the concrete of original aggregate. Among the recycled aggregates, that of pulse-discharged has the higher density and the lower absorption.

Table. 1 Properties of coarse aggregate

Type of recycled aggregate	Saturated density (g/cm^3)	Dried density (g/cm^3)	Water absorption (%)
Crushed	2.53	2.49	2.71
Heated and milled	2.59	2.54	2.10
Pulse discharged	2.95	2.90	1.42
Original	3.06	3.04	0.49

For each aggregate, 3 cylindrical samples were made and tested after 28 day-standard curing. During the compression test, AE measurement was conducted. Silicon grease was pasted on the top and the bottom of the specimen, and a Teflon sheet was inserted to reduce AE events generated by friction. MISTRAS-AE system (PAC) was employed to count AE hits. AE hits were detected by using an AE sensor (UT-1000: 1 MHz resonance frequency). The frequency range was set from 60kHz to 1MHz. An experimental set-up is shown in Figure 6.

Figure 6. AE measurement in the compression test.

For event counting, the dead time was set as 2 msec.. It should be noted that AE measurement was conducted at two channels as well as the measurement of axial and lateral strains. AE hits and strain of the two channels were averaged and estimated as a function of stress level.

3.2 *Corrosion tests*

Reinforced concrete slabs tested were of dimensions 300 mm × 300 mm × 100 mm. Configuration of specimen is illustrated in Figure 7. Reinforcing steel-bars (rebars) of 13 mm diameter are embedded with 15 mm cover-thicknesses for longitudinal arrangement. When making specimens, concrete was mixed with NaCl solution. In order to investigate the threshold limit of chloride concentration for corrosion, the lower-bound threshold value (chloride amount 0.3 kg/m^3 of concrete volume, 0.088% mass of cement) prescribed in the code (JSCE, 2001) was taken into consideration. After the standard curing for 28 days in 20°C water, chloride content was measured and found to be 0.125 kg/m^3 in concrete volume (0.036%of mass of cement). Mixture proportion of concrete was the same as that of recycled concrete, but the maximum size of aggregate was 10 mm. A compressive strength at 28 days of the standard curing was 35.0 MPa. Following the standard curing, all surfaces of the slab specimen

were coated by epoxy, except the bottom surface for one-directional diffusion as illustrated in Figure 7.

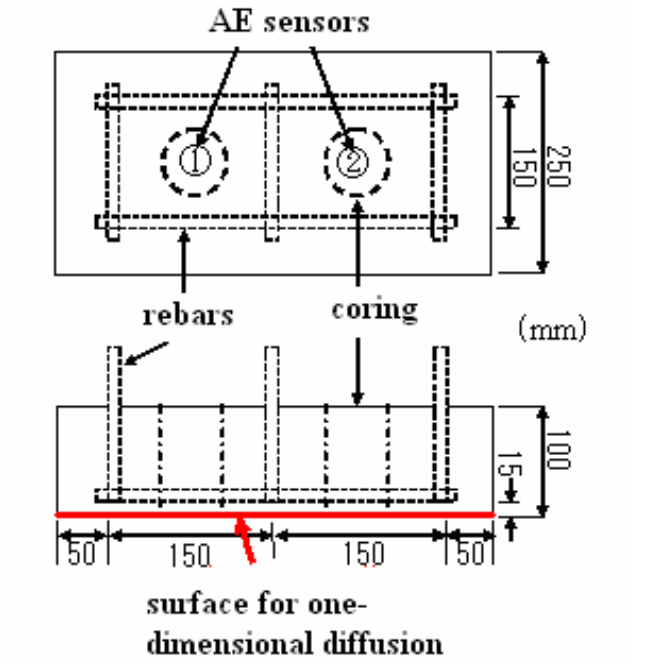

Figure 7. Sketch of a slab specimen.

An accelerated corrosion test and a cyclic wet-dry test were conducted. In the accelerated corrosion test, the specimens were placed on a copper plate in a container filled with 3% NaCl solution as shown in Figure 8. Between rebars and the copper plate, 100 mA electric current was continuously charged. In the cyclic wet-dry test, the specimens were cyclically put into the container in the figure without charge for a week and subsequently dried under ambient temperature for another week.

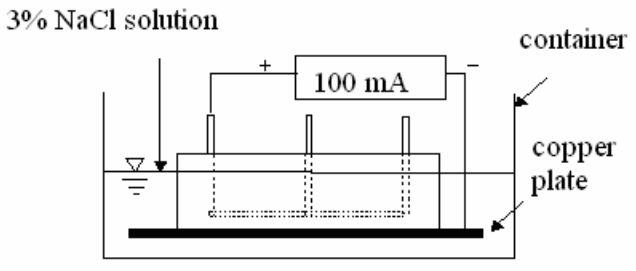

Figure 8. Test set-up for an acceleration test.

AE measurement was continuously conducted, by using LOCAN 320 (PAC). Two AE sensors were attached to the upper surface of concrete at the center of coring locations shown in Figure 7. In order to detect AE signals, a broad-band sensor (UT-1000, PAC) was employed. Frequency range of the measurement was 10 kHz – 1 MHz and total amplifications was 60 dB gain. For event counting, the dead-time was set to 2 msec. with 40 dB threshold.

Half-cell potentials at the surface of the specimen were measured by a portable corrosion-meter, SRI-CM-II (Shikoku Soken, Japan). In the accelerated corrosion test, the measurement was conducted twice a day until the average potentials reached to -350 mV (C.S.E.), which gives more than 90 % possibility of corrosion (ASTM, 1991). In the cyclic test, the specimen was weekly measured until the average potentials in dry condition reached to -350 mV (C.S.E.). During the half-cell potential measurement, AE measurement was discontinured.

Chloride concentrations were measured at several stages. At first, the initial concentration was measured by using a standard cylinder sample after 28-day moisture-curing. At other stages, two core samples of 5 cm diameter were taken from the specimens, of which locations are illustrated in Figure 7. Slicing the core into 5 mm-thick disks and crushing them, concentrations of total chloride ions were determined by the potentiometric titration method.

4 RESULTS AND DISCUSSION

4.1 *Damage evaluation of recycled concrete*

Strengths and moduli of elasticity in four-types of concrete are shown in Figure 9. These are averaged values of three samples for each aggregate. It is found that the strengths of recycled aggregate and the moduli of elasticity are lower than that of the original. Among the recycled concrete, concrete of crushed aggregate has the poorest properties, because a thin mortar-layer is still stuck to the interface with aggregate.

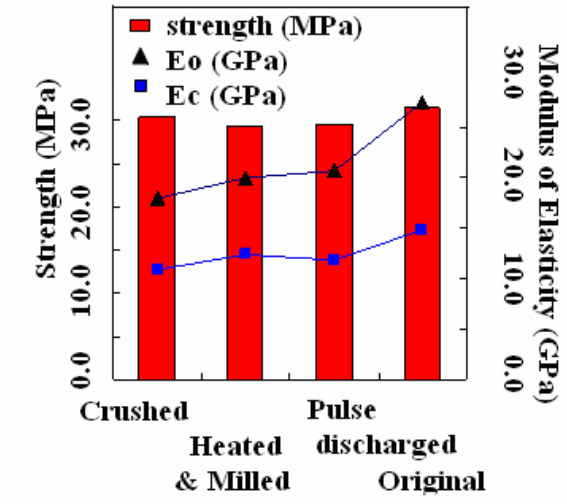

Figure 9. Strength and modulus of elasticity.

From Equation 8, the intact modulus of elasticity, E^*, for each aggregate was evaluated as an aver-

aged value of three samples. Then, as relative damage the ratios of initial moduli E_0 to intact moduli E^* are evaluated. Results are given in Figure 10.

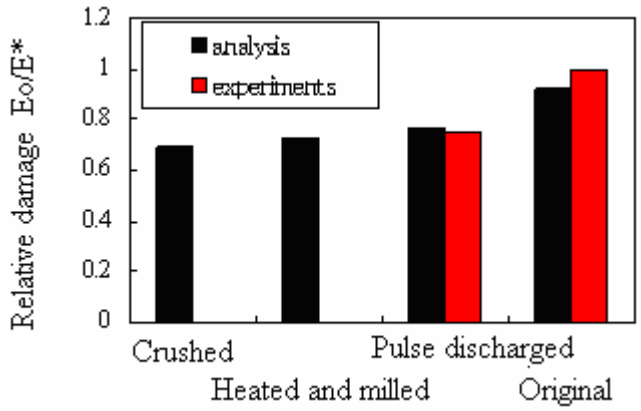

Figure 10. Relative damages of recycles aggregate.

As mentioned before, experimental values are only available for concrete of pulse-discharged and original aggregates. In the figure, a mechanical property of recycle aggregate is evaluated as the relative damage. The poorest property is observed in concrete of crushed aggregate. The property of concrete of recycled aggregate by the pulse-discharged method is better than that of heated and milled, but a slightly lower than that of original aggregate. Agreement between results of AE rate process analysis and actual values in the experiments is remarkable. Although the experimental value of concrete of recycled aggregate by the pulse-discharged method was estimated in comparison with that of original aggregate, analytical value was estimated by AE rate process analysis without knowing that of original aggregate. Thus, it is demonstrated that an application of DeCAT system to evaluate the property of recycled concrete is quantitatively effective.

4.2 *Corrosion detection*

4.2.1 *Accelerated corrosion test*

A relation between AE activity and half-cell potentials measured are shown in Figure 11. The number of AE events is plotted as a sum of AE events at two channels counted for one hour. Two periods of high AE activities are observed at around 3 days elapsed and 7 days elapsed. It is noted that the half-cell potentials start to decrease after the 1st activity, but are still higher than -350 mV around at the 2nd activity. Because the half-cell potential lower than -350 mV is prescribed as more than 90% probability of corrosion (ASTM, 1991), results suggest that the corrosion in rebars is detected by AE activity more confidently than the half-cell potential.

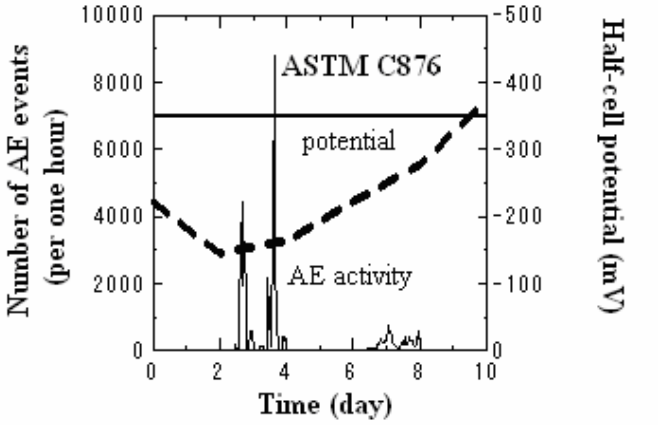

Figure 11. AE activities and half-cell potentials in the accelerated corrosion test.

Total chloride ions were determined in depths, and chloride concentrations at cover thickness were analytically estimated by,

$$C(\mathbf{x},\mathbf{t}) = C_0(1 - erf[\frac{x}{2\sqrt{Dt}}]) \qquad (12)$$

During the test, core samples were taken at four stages, testing all of three specimens. Initially, chloride concentration was measured by using a standard cylindrical sample for the compression test. Following two periods of high AE activities and at the final stage, concrete cores were taken out from the three specimens. Then, chloride concentrations at cover thickness were measured. These experimental values were analyzed by Equation 12 and are compared in Figure 12 (b), where total AE hits observed during the test are compared with chloride concentration at the rebar.

According to a phenomenological model of reinforcement corrosion (Melchers and Li, 2006), typical corrosion loss is reported as illustrated in Figure 12 (a). At phase 1, corrosion is initiated. The rate of the corrosion process is controlled by the rate of transport of oxygen. As the corrosion products build up on the corroding surface of rebar, the flow of oxygen is eventually inhibited and the rate of the corrosion loss decreases as illustrated as phase 2 in Figure 12 (a). This is a nonlinear corrosion-loss-time relationship for corrosion under aerobic conditions. The corrosion process involves further corrosion loss as phases 3 and 4 due to anaerobic corrosion. Accordingly, two stages of active corrosion loss are modeled. In Figure 12 (b), total number of AE hits are plotted, which were obtained from Figure 11. AE activity is compared with chloride concentration at rebar of measured and analyzed values by Equation 12.

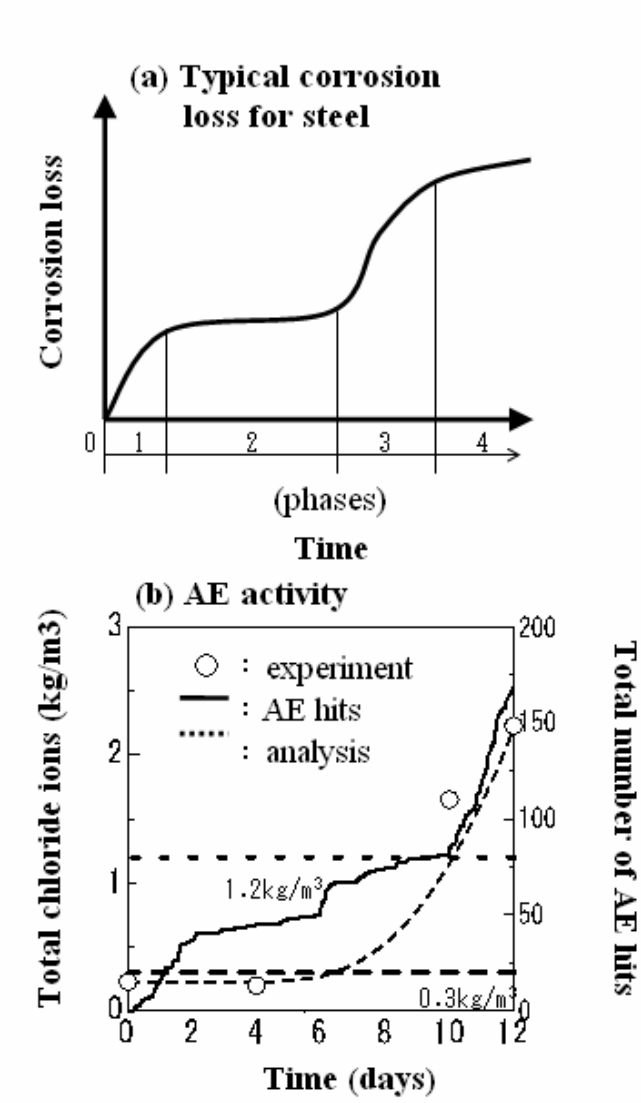

Figure 12. Total number of AE hits and chloride concentration.

It is observed that the increase in total AE hits during the acceleration test is in remarkable agreement with the typical corrosion loss in the phenomenological model. This implies that AE activity clearly corresponds to corrosion activity on the rebar surface. In the figure, two-threshold values of chloride concentration are denoted. One is the lower-bound threshold for the onset of corrosion (0.3 kg/m^3 in concrete volume, 0.088% mass of cement volume) and the other is the threshold value for the performance-based design. According to the code (JSCE, 2001), concrete with chloride content over 1.2 kg/m^3 in concrete volume (0.35 % mass of cement volume) is not accepted for construction to prevent the corrosion. Comparing AE activity with chloride concentration in Figure 12 (b), it is found that chloride concentration becomes higher than 0.3 kg.m^3 after the 1st AE activity, and it reaches over 1.2 kg/m^3 following the 2nd AE activity. This implies that chloride concentrations for corrosion phenomena at rebars reasonably correspond to two-stage high AE activities for the initiation of corrosion and the nucleation of corrosion cracking.

4.2.2 *AE activities in the cyclic tests*

The number of AE events and the half-cell potentials during the cyclic test are shown in Figure 13. The number of AE events for one hour is again plotted. AE events are periodically observed along with cycles of wet and dry. The 1st high AE activity is observed at 40 days elapsed, while the 2nd activity is not obvious. According to the half-cell potentials, the values start to decrease at around 100 days elapsed.

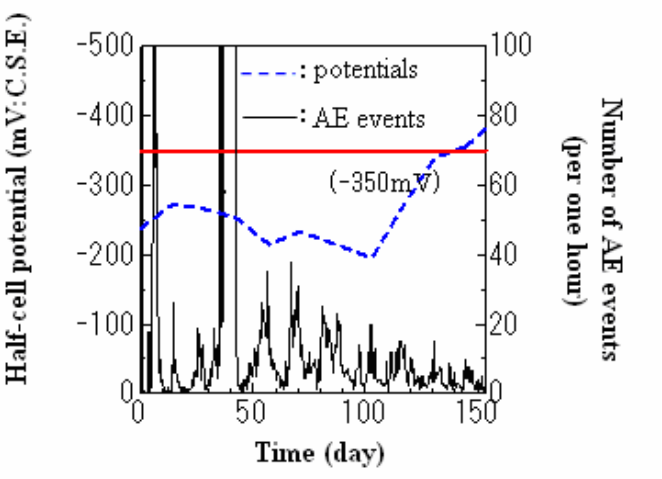

Figure 13. AE activities and half-cell potentials in the cyclic wet-dry test.

In order to identify the period of the 2nd AE activity, the RA values and the average frequency were determined from Equations 9 and 10, averaging the data during two weeks of wet-dry cycles. Results are shown in Figure 14. Corresponding to the 1st period as denoted by an arrow symbol, the RA value becomes large and the average frequency is low. According to Figure 5, AE sources are classified as other than tensile cracks. Toward 100 days elapsed, the increase in the RA value is observed. Thus, the 2nd period is reasonably identified around at 100 days elapsed, where the RA values are low and the average frequencies are fairly high. From Figure 5, tensile cracks are to be nucleated at this period. By analyzing two AE indices of the RA value and the average frequency, the 1st and the 2nd periods of high AE activities are reasonably identified.

The *b*-value was also determined for each wet-dry cycle as the average value. Results are shown in Fig. 15. The *b*-value becomes large at the 1st period (upward arrow symbol) and then the *b*-values keep fairly low. This result implies generation of small cracks of other than a tensile crack around at the 1st period. Then, nucleation of fairly large tensile cracks follows, leading to the 2nd period (downward arrow symbol).

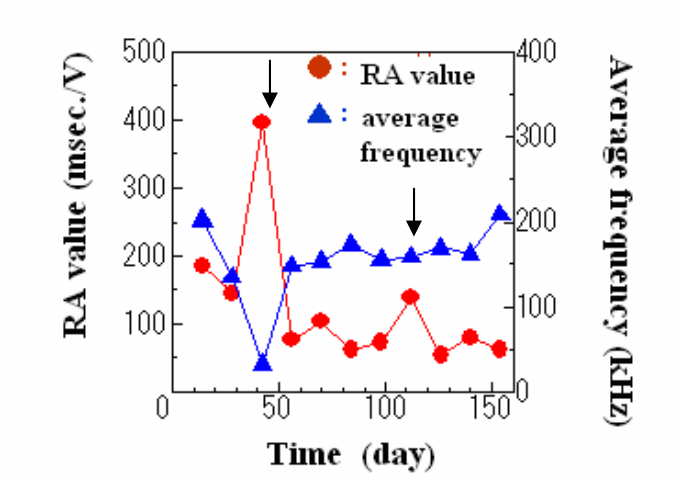

Figure 14. RA values and the average frequencies in the cyclic wet-dry test.

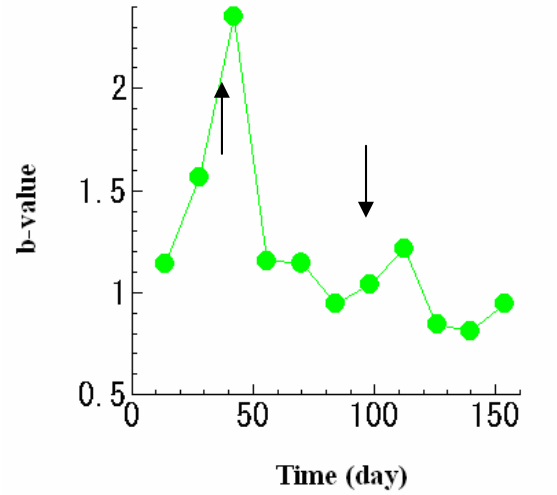

Figure 15. Variation of b-values in the cyclic wet-dry test.

It was found that chloride concentration at rebar reached to the lower-bound threshold of 0. 3 kg/m^3 after 40 days, and at around 100 days elapsed, the concentration became higher than 1.2 kg/m^3. After coring the specimens at 42 days elapsed and 126 days elapsed, rebars were removed and visually inspected. As given in Figure 16, no corrosion was observed after 42 days, while rebar was fully corroded after126 days. These results imply that AE activities after 100 days could reasonably result from concrete cracking due to expansion of corrosive products in rebars, as chloride concentration reached over 1.2 kg/m^3 in concrete.

In order to investigate the condition of rebar at the 1st AE activity in detail, a rebar skin in the left figure of Figure 16 was examined by the scanning electron micrograph (SEM). Distributions of ferrous ions at the initial as received and at 42days elapsed are compared in Figure 17. At the initial stage, homogeneous distribution of ferrous ions is observed, while they disappear at some regions on the surface at 42 days. This implies that onset of corrosion occurs in rebars at the 1st period of AE activities. Although no corrosion was observed visually, rebar were actually corroded as found in the SEM observation.

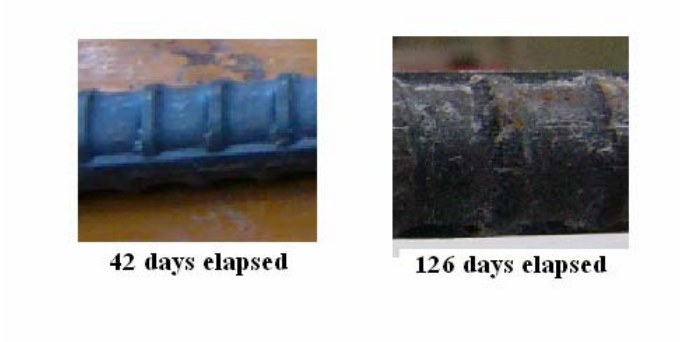

Figure 16. Visual observation of rebars.

Eventually, it is realized that the 1st high AE activity corresponded to the onset of corrosion in the rebars, and the 2nd high AE activity could be generated due to concrete cracking.

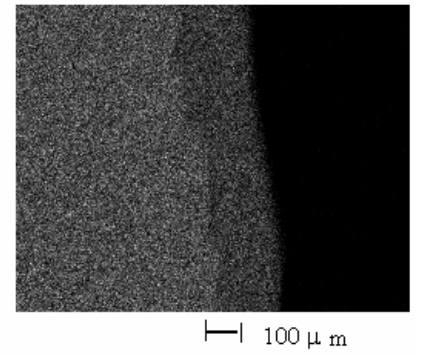

(a) Distribution of ferrous ions (grey region) prior to the test.

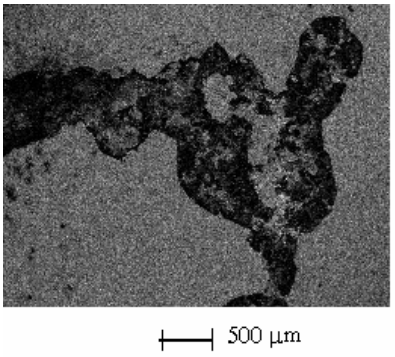

(b) Distribution of ferrous ions (grey region) after the 1st period.

Figure 17. Distributions of ferrous ions on rebar surface.

Comparing these findings with the deterioration process in Figure 1, it is reasonably demonstrated that two key periods in the corrosion process can be identified by AE monitoring. At the onset of corrosion in rebar, small AE events of the other-type cracks are actively observed. At nucleation of cracking in concrete, tensile cracks are generated as

fairly large AE events, which result from cracking in concrete due to expansion of corrosive products.

5 CONCLUSIONS

In the first half of the paper, the quantitative evaluation of damage in concrete is proposed by applying the AE rate-process analysis and damage mechanics. The technique is developed as the DeCAT software. We have the following conclusions.

(1) The relative damage is evaluated by the ratio of the initial modulus of elasticity to the intact modulus, obtained from the DeCAT analysis.

(2) The analysis is applied to evaluate the mechanical property of recycled concrete. Recycled aggregate were obtained by crushing, heated and milled, and pulse-discharged. Making cylindrical concrete samples of similar mix proportions, the compression test of the samples were conducted. Relative damages evaluated are in reasonable agreement with actual deterioration degrees of recycled concrete.

(3) The experimental value of concrete of recycled aggregate by the pulse-discharged method was compared with that of original aggregate as the relative damage. It is confirmed that the relative damage of the analytical value, which was estimated by the DeCAT analysis without knowing that of original aggregate, is in remarkable agreement with the experimental value.

In the second half, the application of continuous AE monitoring in the corrosion process is studied. Because high AE activities are observed in the corrosion process, AE parameters of the RA value and the average frequency were estimated, along with the *b*-vale of AE amplitude distribution Ingress of chloride ions was measured and analyzed, comparing with AE results. We have the following conclusions.

(4) At the 1st period of high AE activities, the RA values become high, the average frequencies are low and the *b*-value is large. This implies that small shear cracks are actively generated as AE sources. Approaching to the 2nd period, the RA values become low, the average frequencies are getting higher and the *b*-values are small. The fact reasonably suggests that fairly large tensile cracks are generated due to expansion of corrosive products.

(5) Compared with AE results, it is found that the onset of corrosion starts, when the chloride concentration exceeds the lower-bound threshold. Nucleation of corrosion cracking is observed, when the chloride concentration becomes over the threshold level specified in the codes.

(6) Removing rebars from the specimen, it is confirmed that rebars could corrode after chloride concentration reaches over the specified threshold, and AE activities after 100 days result from concrete cracking due to expansion of corrosive products in rebars.

(7) In order to investigate the condition of rebars at the 1st activity, a rebar skin was examined by the scanning electron micrograph (SEM). It is found that ferrous ions have disappeared. This suggests that the onset of corrosion occurs in rebars at the 1st period of high AE activities.

(8) These findings demonstrate that two key periods in the corrosion process can be identified both at the onset of corrosion and at the nucleation of cracking by continuous AE monitoring.

REFERENCES

ASTM. 1991, *Standard Test Method for Half-Cell Potentials of Uncoated Reinforcing Steel in Concrete,* ASTM C876.

JCMS. 2003, *Monitoring Methods for Active Cracks in Concrete by A E,* JCMS-II B5706.

JSCE. 2001. *Standard Specifications for Concrete Structures – Version of Maintenance*

Loland, K.E. 1980. Continuous Damage Model for Load – Response Estimation of Concrete", *Cement and Concrete Research* , Vol.10, 395-402.

Melchers, R. E. and Li,, C. Q. 2006. Phenomenological Modeling of Reinforcement Corrosion in Marine Environments, *ACI Materials Journal,* Vol. 103, No. 1, 25-32.

Ohtsu, M. 1992. Process Analysis of Acoustic Emission Activity in Core Test of Concrete", *Proc. of JSCE,* No.442/V-16, 11-217.

Shiotani, T. Ohtsu, M. and Ikeda, K. 2001. Detection and Evaluation of AE Waves due to Rock Deformation, *Construction and Building Materials,* Nos. 5-6**,** 235-246.

Suzuki, T. and Ohtsu, M. 2004, Quantitative Damage Evaluation of Structural Concrete by a Compression Test based on AE Rate Process Analysis, *Construction and Building Materials,* 18, 197-202.